Supporting Information for

Sweet and Blind Spots in E3 Ligase Ligand Space Revealed by a Thermophoresis-Based Assay

Samuel Maiwald[‡], Christopher Heim[‡], Birte Hernandez Alvarez and Marcus D. Hartmann*

Department of Protein Evolution, Max Planck Institute for Developmental Biology, Max-Planck-Ring 5, 72076 Tübingen, Germany

[‡] these authors contributed equally

* correspondence to
M. D. Hartmann,
Tel. +49 7071 601 323,
marcus.hartmann@tuebingen.mpg.de

The impact of DMSO competition on the characterization of CRBN ligands

Owing to their limited solubility, most studies on CRBN ligands are performed in presence of a low percentage of DMSO, typically in the range of 0.2 - 1.0 % [1-5]. This is an intrinsic complication, as DMSO itself is competing with CRBN binders [6]. Consequently, strictly speaking, in every assay performed in presence of DMSO, the test compound is constantly in competition with the latter, independent of the assay technique (e.g. ITC, FP, FRET or MST). Although our measurements in presence of 0.5 % DMSO yielded clean and well-interpretable MST profiles for hTBD, there is also a DMSO-related dampening effect apparent in the raw traces for the thalidomide::hTBD titration (Figure 2), which results from the out-competition of the reporter BODIPY-uracil by DMSO. This dampening is especially visible at the lower concentrations of thalidomide, thus reducing the overall signal amplitude of the titration series. While the nature of MST experiments makes this effect easily appreciable from the raw traces, it is not necessarily obvious from the raw data in other experimental setups, and to the best of our knowledge, the competition of DMSO for CRBN binders has so far not been examined in the literature.

To quantify the effect of this DMSO competition, we performed comparative experiments with the water-soluble CRBN ligands succinimide, uracil and methyluracil, each both in absence and in presence of 0.5 % DMSO (Figure S2). These measurements indicated, that the presence of 0.5 % DMSO leads to a systematic underestimation of the affinity (or overestimation of the IC_{50}) of about 20%; the magnitude of this underestimation only depends on the employed DMSO concentration. Consequently, all K_d and K_i values derived in this and all previous and future studies on CRBN ligands in presence of DMSO would need to be corrected by an appropriate factor - here about 0.8 - independent of the assay technique. As the 0.5 % DMSO employed here can be regarded as representative for most studies on CRBN, we decided to not account for the DMSO competition for better comparability with the literature.

The influence of fluorescence quenching and autofluorescent test compounds

In principle, the fluorescence quenching observed upon BODIPY-uracil::CRBN complex formation used to evaluate the reporter affinity is also present, albeit in a reduced form, in competition experiments. To investigate whether this influences the measurement, we recorded the thermophoretic behavior of BODIPY-uracil at varying concentrations (producing fluorescence intensities similar to those measured in binding experiments), but did not observe an effect on MST behavior (Figure S1). This indicates an increased tolerance towards overlapping optical properties mediated by fluorescence normalization, which is a significant advantage of this assay setup compared to purely fluorescence-based methods.

Further, to estimate the influence of fluorescent test compounds, we performed an experiment in which we titrated a mixture of the ligand succinimide and the fluorescent NT.495 BLUE dye against the BODIPY-uracil::hTBD complex, thus simulating a fluorescent compound. The resulting dose-response curve remained largely unaffected, except for those data points where initial fluorescence exceeded the detector limit, and could be evaluated to an IC_{50} close to that obtained for succinimide under normal conditions (Figure S1). We therefore conclude that the assay is well suited to detect and quantify binding of reasonably potent binders with optical properties that are overlapping with the fluorescent readout of the assay setup.

Experimental Procedures

Cloning

The genes for VHL^{54-213} fused to an N-terminal TwinStrep-tag via a TEV protease cleavage site (VHL), $Elongin\text{-}B^{1-104}$ (EloB) and $Elongin\text{-}C^{17-112}$ (EloC) were codon-optimized, synthesized (Synbio Technologies) and cloned into pET28a for VHL and pETDuet-1 for EloB and EloC, respectively.

The coding sequence for hTBD ($hCRBN^{319-425}$), optimized for expression in *E.coli,* was amplified from an existing vector [6] and cloned into pGEX4T1 via BamHI and XhoI, yielding a thrombin-cleavable N-terminal GST fusion construct. Sequence was confirmed by Sanger sequencing.

Protein Expression and Purification

The VHL/EloB/EloC complex (VBC) was expressed in BL21(DE3) cells. A preculture from one colony of BL21(DE3), cotransformed with the pET28a and pETDuet-1 vectors, was incubated in LB containing 100 µg/ml ampicillin and 50 µg/ml kanamycin at 37 °C overnight. The preculture was diluted 1:100 into LB supplemented with 100 µg/ml ampicillin and 50 µg/ml kanamycin and incubated at 37 °C until OD_{600} reached 0.7, at which point expression was induced with 0.3 mM IPTG. Cultures were incubated at 25 °C for 19 h, and harvested by centrifugation at 6500 xg for 15 min. Cells were resuspended in lysis buffer (20 mM Tris pH 8, 150 mM NaCl, 4 mM $MgCl_2$, DNAse I, Roche cOmplete protease inhibitor) and lysed by sonication. Cell debris was removed by centrifugation at 30.000 xg for 45 min, and the supernatant was loaded on a Streptactin XT high capacity column. After washing with buffer W (100 mM Tris pH 8, 150 mM NaCl, 1 mM EDTA), the protein was eluted using buffer BXT (100 mM Tris pH 8, 150 mM NaCl, 1 mM EDTA, 50 mM Biotin). The TwinStrep-tag was cleaved by digestion with TEV protease at 4 °C overnight. To isolate the VBC complex, the sample was loaded on a Superdex 75 26/60 prep grade column equilibrated with VBC buffer (20 mM bis-Tris pH 7, 150 mM NaCl, 1 mM DTT). Fractions containing VBC were pooled, concentrated, flash-frozen in LN_2 and stored at -80 °C.

hTBD was expressed and purified as described [3], with small modifications: The GST fusion construct was expressed in Rosetta 2(DE3)pLysS, and purified by GSH affinity chromatography (GSTrap HP) followed by cleavage with thrombin and size exclusion chromatography (Superdex 75 26/60).
MsCI4 and MsCI4$^{WW/FF}$ were expressed and purified as described previously [6].

Fluorescence polarization and FRET spectroscopy

FP experiments were performed with the VBC complex as described previously [7], on a Biotek Synergy H4 Hybrid reader.
FRET assay measurements for UMP, nitrofurantoin and avadomide were performed with MsCI4$^{WW/FF}$ using MANT-uracil as described previously [6].

Microscale thermophoresis

The short reporter peptide FAM-DEALA-Hyp-YIPMD (FAM-11mer) and long reporter peptide FAM-DEALA-Hyp-YIPMDDDFQLRSF (FAM-19mer) as well as their unlabeled counterparts (11mer and 19mer) were obtained by custom peptide synthesis (GeneCust; Purity > 98 % as assessed via RP-HPLC). BODIPY-uracil was obtained by custom synthesis (Jena Bioscience; Purity > 99 % as assessed via RP-HPLC). All other compounds were obtained from commercial suppliers at highest available purity (Sigma-Aldrich: succinimide (98.3%), DMSO (100%), rolipram (99.3%), thiohydantoin (99.7%), 4-imidazolidinone (>95%), hydantoin (98%), 1-aminohydantoin (99.5%), nitrofurantoin (99%), 2-NP-AHD (100%), uracil (99.8%), uridine (100%), uridine 5'-monophosphate (99.8%), 1-methyluracil (100%); Cayman Chemicals: iberdomide, azumolene, dasabuvir (>98%); Selleckchem: lenalidomide (99.8%), pomalidomide (99.1%), avadomide (99.2%); TCI chemicals: thalidomide (99.3%); Alfa Aesar: 1-methylhydantoin (97%); Matrix Scientific: 1-(3-(5-nitrofuran-2-yl)allylidene) amino)hydantoin (>95%); LKT labs: sofosbuvir (>98%)) and used without further purification. 11mer, 19mer and BODIPY-uracil were dissolved to 100 mM and further diluted to 1 mM (11mer and 19mer) or 2 mM (BODIPY-uracil) in DMSO. Any further dilutions were done in MST buffer (50 mM Tris pH 7.4, 150 mM NaCl, 10 mM $MgCl_2$, 0.05 % Tween-20, 1 mM TCEP).
For initial K_d determination, 16-point 1:1 dilution series of protein in its respective buffer (VBC buffer for VHL; 20 mM Tris pH 7.5, 150 mM NaCl, 5 mM 2-mercaptoethanol for MsCI4; 50

mM HEPES pH 7.5, 200 mM NaCl, 0.1 mM TCEP for hTBD) were generated and mixed 1:1 with the corresponding reporter, to obtain a final reporter concentration of 20 nM for FAM-11mer and FAM-19mer, and 200 nM for BODIPY-uracil.

For competitive measurements, water-soluble compounds (11mer, 19mer, succinimide, DMSO, hydantoin, 1-methylhydantoin, thiohydantoin, aminohydantoin, 4-imidazolidinone, uracil, uridine, UMP, 1-methyluracil) were titrated directly in water. For compounds dissolved in DMSO (all other compounds), a master dilution series in DMSO was generated and subsequently diluted 1:100 in water to yield a final constant concentration of 0.5 % (v/v) DMSO. Protein and reporter diluted in MST buffer were added in a 1:1 ratio, with final assay concentrations of 570 nM VBC/20 nM FAM-11mer, 80 nM VBC/20 nM FAM-19mer, 3.5 µM MsCI4/200 nM BODIPY-uracil and 10 µM hTBD/200 nM BODIPY-uracil. Samples were mixed by pipetting and loaded in Standard capillaries (NanoTemper). With the exception of very weak or non-binding compounds, triplicates of each compound, meaning three independent dilution series, were measured, if not stated otherwise.

The Z'-Factor was determined using 50 µM thalidomide (including 0.5 % DMSO) as the positive control and 0.5 % DMSO as the negative control. 32 samples of each were measured, with hTBD and BODIPY-uracil at standard assay concentrations.

For the control experiments, the influence of fluorescence quenching was investigated by measuring BODIPY-uracil fluorescence at concentrations ranging from 100 nM to 400 nM in 20 nM increments, generated by individual dilution of 800 nM BODIPY-uracil in MST buffer. To examine the effect of compound autofluorescence, a solution of 2 mM succinimide and 6.5 µM NT.495 BLUE dye (with 1 % residual DMSO) was generated and titrated in 1 % DMSO. For DMSO influence measurements, stock solutions of succinimide, 1-methyluracil and uracil in 1 % DMSO were generated and subsequently titrated in 1 % DMSO. Further processing and measurement of these dilution series was performed as described above.

All measurements were performed on a NanoTemper Monolith NT.115 with a Nano BLUE detector, using MO.Control v1.6 with MST power set to Medium and Temperature Control set to 25 °C. Excitation Power was set to 40 % for VHL and 20 % for MsCI4 and hTBD measurements.

Data were analyzed using PRISM 8, based on on-time 20s unless stated otherwise. Raw normalized fluorescence (F_{norm}) data was baseline-corrected by subtracting the mean of the normalized fluorescence values measured for the lowest compound concentration. The baseline corrected F_{norm} (ΔF_{norm}) was plotted against the log of compound concentration and fitted using a nonlinear four-parameter fit. For simplicity, only the larger part of the asymmetrical 95 %

confidence interval for the IC_{50} is given. For only weakly binding compounds where the fit yielded an IC_{50} greater than the highest assay concentration, the IC_{50} was reported as higher than that concentration. Conversion of IC_{50} values to K_i values was achieved as described previously [8]. K_i error values were calculated as the difference between the K_i and a theoretical K_i calculated from the lower boundary of the IC_{50} 95 % confidence interval.

Supplementary Figures

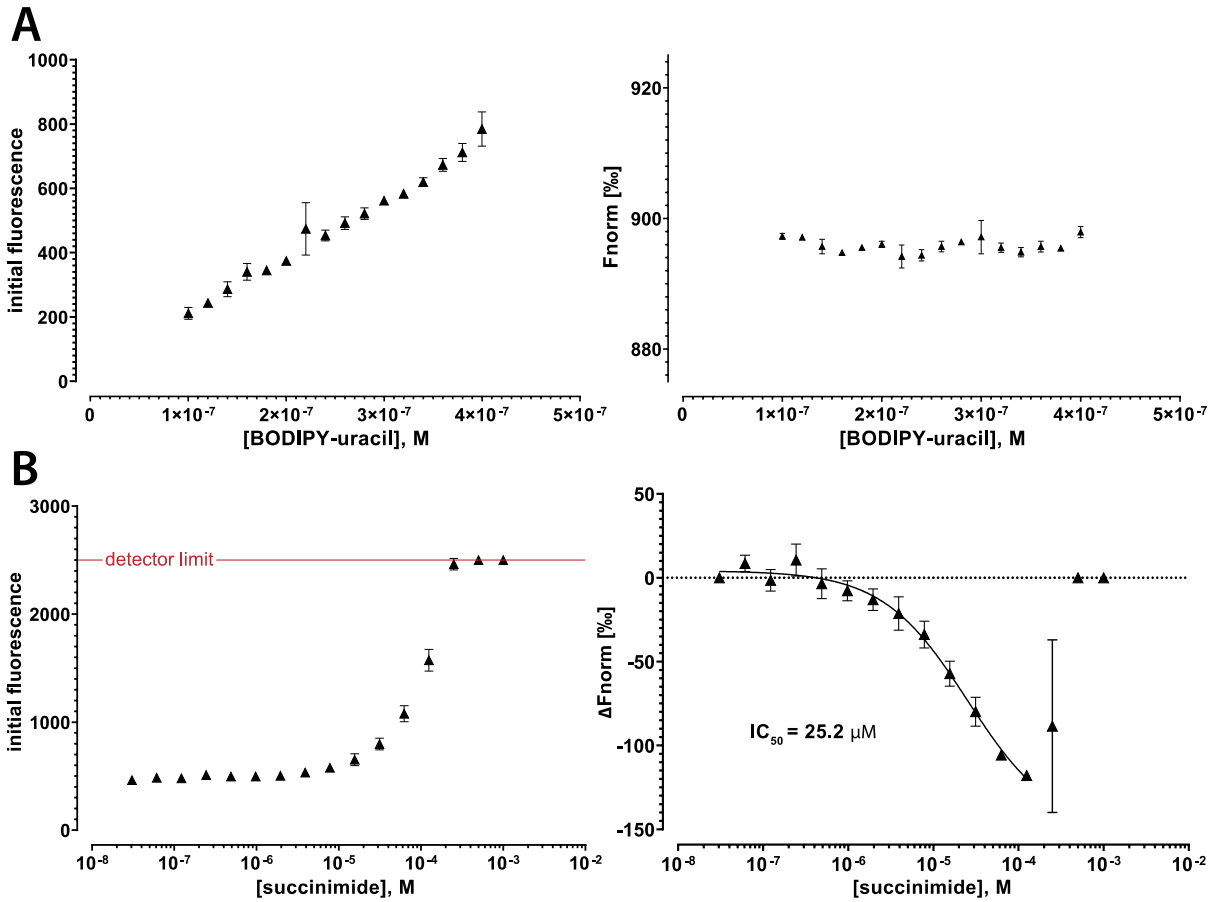

Figure S1: Influence of initial fluorescence on MST behavior. **A** Initial fluorescence and normalized fluorescence at on-time 20 s for varying concentrations of BODIPY-uracil. **B** Initial fluorescence and dose-response curve for titration of succinimide with NT.495 BLUE dye against BODIPY-uracil::hTBD (n = 2); for 0.25 mM succinimide, fluorescence intensity of one replicate exceeded the detector limit while the other did not, resulting in a large difference in ΔF_{norm}.

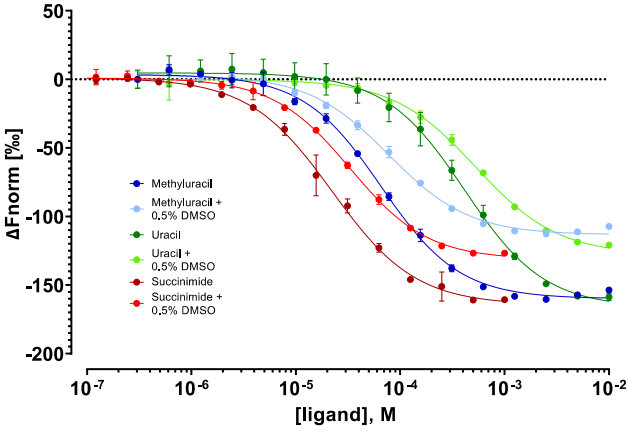

compound	IC_{50} [µM]	IC_{50} (0.5% DMSO) [µM]	Rel. Dev. [%]
succinimide	22.3	33.3	33.0
methyluracil	65.7	77.9	15.7
uracil	415	529	21.6

Figure S2: Influence of DMSO. Dose-response curves and IC_{50} values for succinimide, 1-methyluracil and uracil in absence and presence of 0.5 % DMSO.

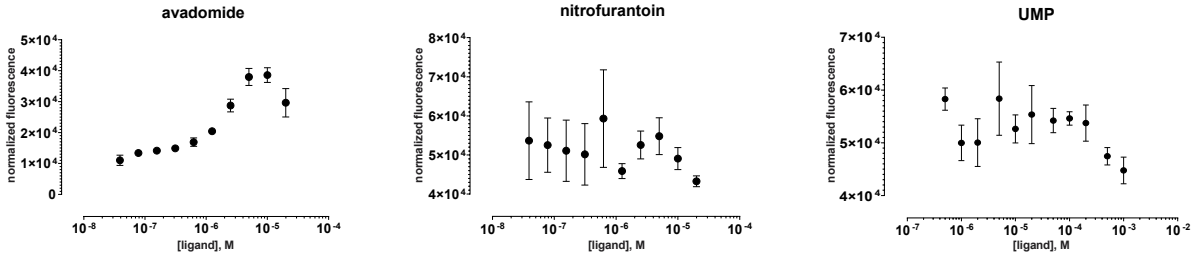

Figure S3: FRET assay data showing normalized fluorescence for titrations of avadomide, nitrofurantoin and UMP. Avadomide shows inverse behavior of fluorescence owed to its own fluorescence at the monitored wavelength so that binding could not be evaluated. Nitrofurantoin and UMP do not show binding. All measurements are based on MsCI4.

Supplementary References

1. Fischer, E. S.; Bohm, K.; Lydeard, J. R.; Yang, H.; Stadler, M. B.; Cavadini, S.; Nagel, J.; Serluca, F.; Acker, V.; Lingaraju, G. M.; Tichkule, R. B.; Schebesta, M.; Forrester, W. C.; Schirle, M.; Hassiepen, U.; Ottl, J.; Hild, M.; Beckwith, R. E.; Harper, J. W.; Jenkins, J. L.; Thoma, N. H., Structure of the DDB1-CRBN E3 ubiquitin ligase in complex with thalidomide. *Nature* **2014,** *512* (7512), 49-53.
2. Mori, T.; Ito, T.; Liu, S.; Ando, H.; Sakamoto, S.; Yamaguchi, Y.; Tokunaga, E.; Shibata, N.; Handa, H.; Hakoshima, T., Structural basis of thalidomide enantiomer binding to cereblon. *Sci Rep* **2018,** *8* (1), 1294.
3. Akuffo, A. A.; Alontaga, A. Y.; Metcalf, R.; Beatty, M. S.; Becker, A.; McDaniel, J. M.; Hesterberg, R. S.; Goodheart, W. E.; Gunawan, S.; Ayaz, M.; Yang, Y.; Karim, M. R.; Orobello, M. E.; Daniel, K.; Guida, W.; Yoder, J. A.; Rajadhyaksha, A. M.; Schonbrunn, E.; Lawrence, H. R.; Lawrence, N. J.; Epling-Burnette, P. K., Ligand-mediated protein degradation reveals functional conservation among sequence variants of the CUL4-type E3 ligase substrate receptor cereblon. *J Biol Chem* **2018,** *293* (16), 6187-6200.
4. Furihata, H.; Yamanaka, S.; Honda, T.; Miyauchi, Y.; Asano, A.; Shibata, N.; Tanokura, M.; Sawasaki, T.; Miyakawa, T., Structural bases of IMiD selectivity that emerges by 5-hydroxythalidomide. *Nat Commun* **2020,** *11* (1), 4578.
5. Powell, C. E.; Du, G.; Che, J.; He, Z.; Donovan, K. A.; Yue, H.; Wang, E. S.; Nowak, R. P.; Zhang, T.; Fischer, E. S.; Gray, N. S., Selective Degradation of GSPT1 by Cereblon Modulators Identified via a Focused Combinatorial Library. *ACS Chem Biol* **2020,** *15* (10), 2722-2730.
6. Boichenko, I.; Deiss, S.; Bar, K.; Hartmann, M. D.; Hernandez Alvarez, B., A FRET-Based Assay for the Identification and Characterization of Cereblon Ligands. *J Med Chem* **2016,** *59* (2), 770-4.
7. Buckley, D. L.; Van Molle, I.; Gareiss, P. C.; Tae, H. S.; Michel, J.; Noblin, D. J.; Jorgensen, W. L.; Ciulli, A.; Crews, C. M., Targeting the von Hippel-Lindau E3 ubiquitin ligase using small molecules to disrupt the VHL/HIF-1alpha interaction. *J Am Chem Soc* **2012,** *134* (10), 4465-8.
8. Nikolovska-Coleska, Z.; Wang, R.; Fang, X.; Pan, H.; Tomita, Y.; Li, P.; Roller, P. P.; Krajewski, K.; Saito, N. G.; Stuckey, J. A.; Wang, S., Development and optimization of a binding assay for the XIAP BIR3 domain using fluorescence polarization. *Anal Biochem* **2004,** *332* (2), 261-73.